

Circumstellar envelope manifestations in the optical spectra of evolved stars

V.G. Klochkova

Special Astrophysical Observatory RAS, Nizhnij Arkhyz, 369167 Russia

July 17, 2018

Abstract We consider the peculiarities of the optical spectra of far evolved stars with circumstellar gaseous–dusty envelopes: the time variability of the absorption–emission profiles of the $H\alpha$ line, the presence of stationary emission and absorption molecular bands, multicomponent complex profiles of the Na I D–doublet lines. We show that the peculiarities of the line profiles (the presence of an emission component in the Na I D doublet lines, the specific type of the molecular features, the asymmetry or splitting of the profiles of strongest absorptions with low excitation potential of the low level) can be associated with the kinematic and chemical properties of the circumstellar envelope and its morphological type.

1. INTRODUCTION

In this paper we analyze the features of the optical spectra of far evolved stars that form in extended gas and dust envelopes. The main targets of the studied sample are protoplanetary nebulae (PPN)—objects at the post-asymptotic branch (post-AGB) stage of evolution, as well as some related stars with large infrared excesses. On the Hertzsprung–Russell diagram stars undergoing the short-lived PPN stage evolve from the asymptotic giant branch toward the planetary nebula (PN) stage at almost constant luminosity, getting increasingly hotter in the process. These descendants of AGB stars are low-mass cores with typical masses of $0.6 M_{\odot}$ surrounded by an extended and often structured gaseous envelope, which formed as a result of substantial mass loss by the star during the preceding evolutionary stages. AGB and post-AGB stars are popular among both theorists and observers because it is during these evolutionary stages that the synthesis and subsequent dredge-up (third mixing) of carbon and heavy s–process metals [1, 2] occur. AGB stars are therefore the principal suppliers of heavy metals and important suppliers of carbon and nitrogen to the interstellar medium [3], thereby participating in the chemical evolution of galaxies.

Furthermore, AGB and post-AGB stars also owe their popularity to the fact that they can serve as tools for the study of stellar-wind manifestations. The mass loss of evolved stars is the dominating factor of the final stages of stellar evolution. The specifics of mass loss (mass-loss rate, sequence of wind episodes, interaction of stellar winds, and details of the chemical composition of the upper outflowing layers) determine the chemical composition and structure of the circumstellar envelopes that form around protoplanetary and planetary nebulae. The stellar-wind history thus remains recorded in the shape, structural features, and chemical peculiarities of the circumstellar envelope.

However, the details of the mass loss process during the AGB–PN transition remain unclear. This is primarily true for the physical processes that shape the complex structure of PPN envelopes. Images taken with the Hubble Space Telescope [4, 5] and during space IR missions [6] are rarely spherical. Central stars are usually surrounded by envelopes in the form of extended haloes, arcs, lobes, and tori. Some stars exhibit various combinations of the above features as well as bipolar and quadrupolar nebulae with dust bars. Examples of the latter two types include the Egg = RAFGL 2688 and IRAS 19475+3119 nebulae, for which high-resolution images were taken by the Hubble Space Telescope [7]. All PPNe and about 80% of planetary nebulae are asymmetric [8]. Much remains to be understood about the processes of condensation of dust particles and formation of the dust fraction in AGB star envelopes (see [9] and references therein).

A circumstellar gas and dust envelope shows up in the form of peculiarities in the IR, radio, and optical spectra of post-AGB supergiants. The optical spectra of PPNe differ from those of classical massive supergiants by the presence of molecular bands superimposed onto the spectrum of an F–G supergiant and by the anomalous behavior of the profiles of selected spectral features. These may include complex emission and absorption profiles of H I, Na I, and He I lines, profiles of strong absorptions distorted by emissions or splitting, and metal emission features. Furthermore, all these peculiarities are variable.

In this paper we analyze the manifestations of circumstellar envelopes in the optical spectra of PPNe paying special attention to the stars whose atmospheres, according to previous studies, underwent evolutionary variations of the chemical composition. Section 2 briefly describes the employed observational data and lists the studied stars and their basic parameters. In addition to PPNe, we also study several related luminous stars with similar properties, including objects with unclear evolutionary status. In Section 3 we analyze the available data on the peculiarities of the profiles of the H α , Na I doublet, and metal lines, found in high-resolution spectra, as well as data on the presence of molecular bands and outflow velocities for objects with different envelope structures. In Sections 4 and 5 we discuss the obtained results and summarize the main conclusions.

2. OBSERVATIONAL DATA

Over the past decade AGB and post-AGB supergiants with IR excesses and several luminous stars with unclear evolutionary status have been spectroscopically monitored with the 6-m telescope of the Special Astrophysical Observatory (V.G. Klochkova). As a result, a collection of high-quality spectra has been acquired with the primary purpose of searching for anomalies of stellar chemical composition due to the nucleosynthesis of chemical elements in the interiors of low- and intermediate-mass stars (with masses smaller than $8 \div 9M_{\odot}$) and the subsequent dredge-up of the synthesis products to the surface layers of stellar atmospheres. These observational data are also used to search for peculiarities in the PPN spectra, to analyze the velocity fields in the atmospheres and envelopes of these stars with mass loss, and to search for the likely long-term spectral and velocity-field variations.

Table 1. List of supergiants of various types studied. We adopt the types and spectral types of the objects from the SIMBAD database. The last column lists the references to the papers reporting the main results for the corresponding objects, including their effective temperatures.

Star	IRAS	Type of object	Sp	T_{eff} , K	References
EM VES 695	00470+6429	emission	B2–3		[10]
GSC 04501–00166	01005+7910	PPN	B2 Iab:e	21500	[11]
XX Cam		R CrB ¹	G Iab:e	7250	[12]
GSC 02381–01014	04296+3429	PPN	G0 Ia	6300	[13]
BD +48°1220	05040+4820	PPN	A4 Ia	7900	[14, 15]
BD –6°1178	05238–0626	var?	F5 III + F3 IV		[16]
HD 56126	07134+1005	puls SR ²	F5 Iab	6600	[17, 18]
St H α 62	07171+1823	emission	B0.5 I	21000	[19]
AI CMi	07331+0021	puls	G5 Iab	4500	[20]
V510 Pup	08005–2356	puls SR	F5 Iae	7300	[21]
HD 82040	09276+4454	binary	M6	3400	[22]
LN Hya	12538–2611	puls SR	F3 Ia		[23, 24]
Z UMi	15060+8315	var Mira ³		5250	[25]
R CrB	15645+2818	var, carb	G0 Iab:pe		[26]
UU Her		puls SR	F2 Ib	6200	[27, 28]
M12 K 413				4800	[29]
M12 K 307		W Vir ⁴		5600	[30]
V4334 Sgr		nova-like	F2-3 II	7250	[31]
V814 Her	17436+5003	puls SR	F3 Ib	7100	[33, 32]
89 Her	17534+2603	puls SR	F2 Ibe		[23]
V886 Her	18062+2410	Be	B1 IIIpe		[34]
V887 Her	18095+2704	puls SR	F3 Ib	6500	[18, 35]
GSC 00439–00590	18123+0511	PPN	G5	4500	[36]
R Sct	18448–0545	RV Tau-type	K0 Ibpv	4500	[37]
HD 179821	19114+0002	puls SR	G5 Ia	5000	[38]
IRC +10420	19244+1115	HG ⁵	F8 I–G0 I	9200	[39, 40]
HD 331319	19475+3119	PPN	F3 Ib	7200	[32]
V5112 Sgr	19500–1709	PPN	F2/F3 Iab	8000	[41, 42]
CGCS 6857	20000+3239	PPN	G8 Ia	5000	[43]
V1027 Cyg	20004+2955	puls	G7 Ia	5000	[44]
QY Sge	20056+1834	puls SR	G0e	6250	[45]
FG Sge	20097+2010	PPN	B4 Ieq–K2 Ib	5500	[46, 47]
V1853 Cyg	20462+3416	puls	B1 Iae	20000	[48]
GSC 01655–00558	20508+2011			4800	[49]
V2324 Cyg	20572+4919	PPN	F0 III	7500	[50]
V1610 Cyg	RAFGL 2688	PPN	F5 Iae	6500	[51, 52]
V448 Lac	22223+4327	puls SR	F9 Ia	6500	[41, 53]
V354 Lac	22272+5435	puls var	G5 Ia	5600	[54, 55, 56]
CGCS 6918	23304+6147	PPN	G2 Ia	5900	[57]
ρ Cas	23518+5713	HG ⁵	G2 Ia0e	5900	[58]

¹ R CrB type variable, ² semiregular variable, ³ Mira, ⁴ W Vir type variable in a globular cluster, ⁵ yellow hypergiant.

Here we use the data acquired in the Nasmyth focus with the NES [59, 60] and Lynx [61] echelle spectrographs. The NES spectrograph, equipped with a 2048×2048 CCD and an image slicer [62], produces a spectroscopic resolution of $R \approx 60\,000$. Since 2011 the NES spectrograph has been equipped with a 2048×4096 CCD which made it possible to significantly extend the wavelength coverage. The Lynx spectrograph, equipped with a 1k×1k CCD, produces a spectroscopic resolution of $R \approx 25\,000$. The spectra of the faintest

program objects (the stars K 307 and K 413 in the globular cluster M 12, V1027 Cyg, V4334 Sgr, the optical components of the IR sources IRAS 04296+3429, 18123+0511, 23304+6147, and other stars with apparent magnitudes $V \geq 13^m$) were acquired with the PFES echelle spectrograph mounted in the primary focus of the 6-m telescope [63].

This spectrograph, equipped with a 1k×1k CCD, produces a spectroscopic resolution of $R \approx 15\,000$. We described the details of spectrophotometric and position measurements of the spectra in our earlier papers, the corresponding references can be found in Table 1.

Note that we had to modify substantially the standard ECHELLE context of the MIDAS system, because of the image slicer employed. We used the software described in [64] to extract the data from the two-dimensional echelle spectra.

Table 2. Basic data for selected post-AGB stars

Object	21 μm	[C/Fe] and [s/Fe]	Morphology of the envelope [5, 4, 7, 8]	Type of the C ₂ bands	V_{exp} , km s ⁻¹	
					CO	optics
02229+6208	+	+	bipolar	abs. [66]	10.7 [67]	8–15 [66]
04296+3429	+	+	bipolar + halo + bar	emiss. [13] abs. [68]	10.8 [67]	3 [13]
05113+1347	+	+	unresolved	abs. [68]	8–10 [69]	6.3 [70]
05341+0852	+	+	elongated halo	no [68] abs. [71]		10.8 [71]
07134+1005	+	+	elongated halo	abs. [68, 72]	10.2 [67]	11 [72]
08005–2356	data unavailable		bipolar	abs. [21] uncertain [68]	100: [73]	42 [21]
12538–2611	–	–	unresolved	no [24]		
19475+3119	–	–	quadrupole + halo	no [32]	16.2, 20.1 [67]	
19500–1709	+	+	bipolar	no [42]	17.2 and 29.5 [67]	20 and 30 [42]
20000+3239	+	+	elongated halo	abs. [68, 43]	12.0 [74]	11.1 [43]
RAFGL 2688	+	+	multipolar + halo + arcs	abs. [68] emiss. [51]	17.9, 19.7 [69]	22.8 [68] 60 [51]
22223+4327	+	+	halo+small lobes	abs. [68] emiss. [53]	14–15 [69]	14.0 [68] 15.2 [53]
22272+5435	+	+	elongated halo + arcs	abs. [56, 68]	9.1–9.2 [67]	10.8 [55] 11.6 [68]
23304+6147	+	+	quadrupole + halo + arcs	abs. [68] emiss. [57]	9.2–10.3 [67]	15.5 [68] ≈ 20 [57]

Carbon [C/Fe] and heavy-metal [s/Fe] overabundance (or lack thereof) in the atmosphere of the central star is indicated by the “+” sign in the third column in accordance with the results of Reddy et al. [66, 70, 71] for IRAS 02229+6208, 05113+1347, and 05341+0852 respectively; Klochkova et al. [13, 18, 21, 32, 57] for IRAS 04296+3429, 07134+1005, 08005–2356, 19475+3119, and 23304+6147 respectively; Klochkova [42] for V5112 Sgr; Kipper and Klochkova [43] for IRAS 20000+3239; Klochkova et al. [52] and Ishigaki et al. [75] for RAFGL 2688; Klochkova et al. [53] Klochkova et al. [55] for V354 Lac. The last column gives the expansion velocity of the envelope for V448 Lac; as determined from the position of C₂ Swan bands. The expansion velocity for IRAS 19500–1709 is determined from the envelope components of the Ba II lines.

3. PECULIARITIES OF THE OPTICAL SPECTRA OF POST-AGB STARS

Our comprehensive study of the program stars allowed us to determine (or refine) their evolutionary status. One of the results of our analysis is that the studied sample of luminous stars with IR-excesses is not homogeneous [65]. It follows from Table 1 that the program objects include luminous stars of various types ranging from low-mass W Vir type variables to hypergiants. In this paper we analyze the peculiarities of the optical spectra of post-AGB stars paying special attention to the subsample of objects listed in Table 2. It contains objects with central stars whose atmospheres are overabundant in carbon and heavy metals and whose circumstellar envelopes have a complex morphology and are usually rich in carbon, as evidenced by the presence of C₂, C₃, CN, CO, etc. molecular bands in their IR, radio, and optical spectra. Furthermore, the objects from Table 2 are among those few PPNe whose IR-spectra exhibit the so far unidentified emission band at 21 μm [77, 76]. Despite an extensive search for appropriate chemical agents, so far no conclusive identification has been proposed for this rarely observed feature. However, its very presence in the spectra of PPNe with carbon enriched envelopes suggests that this emission may be due to the presence of a complex carbon-containing molecule in the envelope (see [76, 78] for details and references).

In addition to a sample of related objects with the above features, Table 2 also includes the infrared sources IRAS 08005–2356, 12538–2611, and 19475+3119. The object IRAS 08005–2356 has so far been poorly studied, and no data are available either on the peculiarities of the chemical composition of its atmosphere or on the presence of the 21- μm band. However, IRAS 08005–2356 can be viewed as related to the objects of this sample because the optical spectrum of its central star V510 Pup exhibits C₂ Swan bands, the hydrogen and metal lines in its spectrum have emission-absorption profiles [21], and the circumstellar envelope is observed in CO emission [73]. The infrared source IRAS 12538–2611 is associated with the high-latitude supergiant LN Hya, which exhibits a number of spectral peculiarities [24] deserving a detailed discussion within the context considered. IRAS 19475+3119 also has a number of exceptional peculiarities, e.g., a strong overabundance of helium in the atmosphere of its central star [32].

The principal types of spectral features in the optical spectra of PPNe are:

1. low- or moderate-intensity metal absorptions, whose symmetric profiles show no apparent distortions;
2. complex profiles of neutral hydrogen lines, which vary with time and include absorption and emission components;
3. the strongest metal absorptions with low excitation potentials of the low level, their variable profiles are often distorted by envelope features that make the profile asymmetric or split it into several components;
4. absorption or emission bands of mostly carbon containing molecules;
5. envelope components of the Na I and K I resonance lines; (6) narrow permitted or forbidden metal emission lines that form in envelopes.

The presence of type 2–6 features is the key difference of the spectra of PPNe from those of massive supergiants.

Our sample of PPNe, thoroughly studied by high-resolution spectra (Table 2), practically coincides with the list of C-rich protoplanetary nebulae the photometric and spectral

properties of which were extensively studied by Hrivnak et al. [76, 79]. Of fundamental importance to us is the conclusion of Hrivnak et al. [80] about the rare occurrence of binaries among post-AGB stars of the type considered, which is based on the long-term investigation of the velocity field in PPN atmospheres conducted by the above authors. Van Winckel [81], on the contrary, finds binary occurrence to be very high among RV Tau type variables with near-IR excesses, which also undergo the post-AGB stage of evolution. Thus, the results of Hrivnak et al. [76, 79, 80] provide further evidence for the homogeneity of the PPN sample considered here.

3.1. $H\alpha$ Line

The $H\alpha$ lines in the spectra of PPNe have complex (they combine emission and absorption components) and variable profiles of various types: profiles with an asymmetric P Cyg type core or inverse P Cyg type profiles with two emission components in the wings. The profiles often combine the features of both types. The presence of emission features in the $H\alpha$ line is indicative of a high mass loss rate [82] and serves as an indicator used for the search and identification of PPNe (see, e.g., a review by Kwok [77]). A good guidance is provided by the atlas of the HD 56126 spectra [72], which illustrates the main features of the optical PPN spectra mentioned above. The combination of observed properties (a typical double-humped spectral energy distribution, F-supergiant spectrum with a variable absorption and emission $H\alpha$ profile, C₂ Swan bands in the optical spectrum that form in the outflowing extended envelope, high overabundance in carbon and s-process heavy metals dredged up to the surface layers of the atmosphere as a result of mixing) makes this object a canonical post-AGB star. The $H\alpha$ profile in the spectrum of this star exhibits a striking degree of variability: it follows from Fig. 2 in the atlas [72] that all the above profile types—symmetric core, direct or inverse P Cyg type profile, and profiles with two emissions in the wings—were observed at different times during decade-long observations with the 6-m telescope.

The complex $H\alpha$ profile in the spectrum of V448 Lac consists of a narrow core and broad wings [53]. According to the classification of Sánchez Contreras et al. [83], this profile can be classified as belonging to the type “EFA” (emission-filled absorption). $H\alpha$ profiles of the same type are observed in PPN spectra irrespective of whether or not the atmosphere of the central star is enriched in carbon and heavy metals. For example, $H\alpha$ lines with EFA profiles have been recorded in the spectra of stars with enriched atmospheres associated with the following sources: IRAS 04296+3429 [13], 05341+0852 [71], 07134+1005 [72], 19500–1709, 22223+4327 [53], and 23304+6147 [57]. Profiles of the same type were also recorded in the spectra of objects with non-enriched stellar atmospheres: IRAS 05040+4820 [15], 18095+2704 [18], and 19475+3119 [32]. We can make a similar conclusion that $H\alpha$ lines with EFA profiles are observed in the spectra of objects with different envelope morphologies.

Figure 1 shows the $H\alpha$ core in the “intensity–radial velocity (V_r)” coordinates as observed in the spectra of V448 Lac taken in 2005 and 2008. This figure illustrates the variability of the $H\alpha$ core, and the radial velocity measurements [53] indicate that the $H\alpha$ core is systematically blue-shifted relative to the metal lines. Klochkova et al. [53] concluded that the profile of this line observed in the spectrum of V448 Lac is inconsistent with the theoretical LTE profile computed assuming normal (solar) hydrogen abundance. This discrepancy suggests that the envelope contributes to the formation of the profile and (or) that the $H\alpha$ formation conditions deviate from LTE. The available combination of the observed properties (effective temperature T_{eff} , luminosity class, light variations, unstable

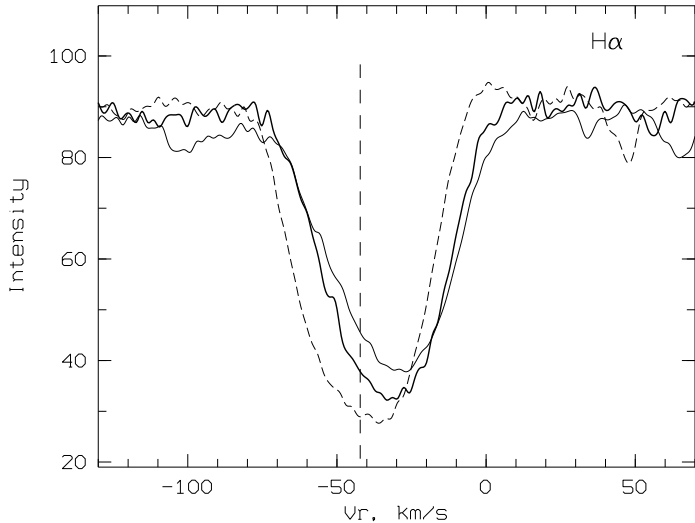


Figure 1. Variability of the core of the $H\alpha$ profile in the spectrum of V448 Lac 53. The vertical dashed line shows the systemic velocity. Here and in the subsequent figures showing parts of the spectra, the intensity along the vertical axis is plotted in relative units I/I_{cont} with the continuum intensity assumed to be equal to 100 units.

behavior of atmospheric line V_r variations, peculiarities of the optical and IR-spectra, including the variable peculiar profile of the $H\alpha$ line, the asymmetry of the strongest absorptions, the combination of molecular bands, the similarity of the elemental abundance pattern in the atmosphere, and similar envelope morphology) is indicative of the analogy between V448 Lac and HD 56126.

A typical example of a profile with two emission components is the $H\alpha$ profile of the high-latitude post-AGB supergiant V5112 Sgr recorded at three observing epochs [42] and shown in Fig. 2. The spectrum of this object, whose envelope even the Hubble Space Telescope failed to resolve [7], exhibits variations of both the intensities and positions of the absorption and emission components of the $H\alpha$ line.

The spectrum of the faint near-AGB optical component of IRAS 20508+2011 shows a different type of profile and a different spectral variability pattern. The powerful extended wings of the profile in Fig. 3 are typical for such a cool supergiant ($T_{\text{eff}} = 4800$ K [49]) at the close to AGB-stage. The $H\alpha$ emission has a variable absorption superimposed on it. According to the classification of Sánchez Contreras et al. [83], the $H\alpha$ profile of this object in our earliest spectra can be classified as type “PE” (pure emission). Sánchez Contreras et al. [83] recorded PE type profiles in the spectra of two AGB objects: IRAS 09452+1330 and 10131+3049. The broad extent of the emission wings is indicative of a high stellar-wind velocity near the AGB-stage. The extent of the $H\alpha$ wings has remained almost unchanged throughout the five years of our observations of IRAS 20508+2011, but nonstationary absorption is gradually becoming the dominating component. Radial velocity measurements [49] showed that the absorption in $H\alpha$ is systematically redshifted by about 10 km s^{-1} relative to the photospheric lines (the position of the absorption in $H\alpha$ is consistent with that of the metal lines only on one observing date). The intensity of the blue-shifted emission exceeds that of the redshifted emission at all observing epochs.

As is evident from Fig. 3, the $H\alpha$ profile in the spectrum of IRAS 20508+2011 changed in 1999–2003 from a powerful bell-like emission with a weak absorption in the core to a two-peaked emission. The emission intensity systematically decreased, and in the spectrum taken in 2003 (profile 3 in Fig. 3) the central absorption was below the continuum level.

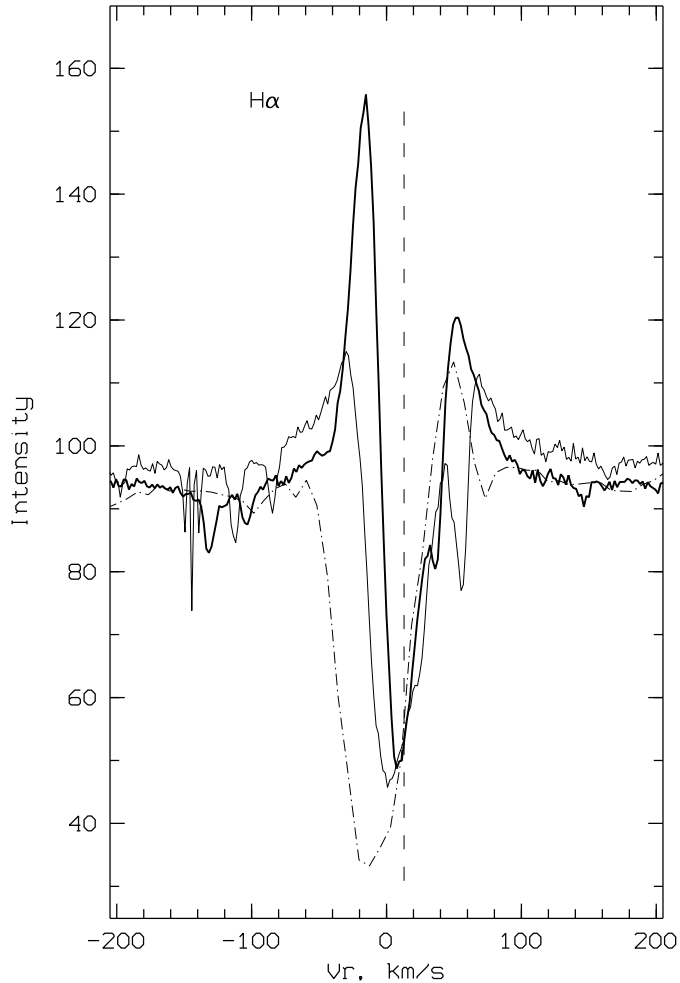


Figure 2. Variability of the absorption and emission profile of the $H\alpha$ line in the spectra of the high-latitude post-AGB supergiant V5112 Sgr [42] taken on different dates: August 2, 2012 (the solid thin line) and September 28, 2010 (the solid bold line). The dash-dotted line shows the profile in the spectrum taken on July 5, 1996 with the LYNX spectrograph with a resolution of $R = 25\,000$ [61]. The vertical dashed line indicates the systemic velocity.

The width of the emission-line wings also changed in the process. The observed $H\alpha$ profile can be interpreted as a superposition of two lines of different nature: a photospheric absorption and a strong emission spanning a wide range of velocities that forms in the extended circumstellar structure. The wings of the resulting emission profile extend out to the radial velocity of $\pm 250 \text{ km s}^{-1}$.

The variability of the $H\alpha$ emission is a well known phenomenon in AGB- and post-AGB stars (see [84, 85] and references therein). The differences in the types of $H\alpha$ profiles and their variations are due to the instability of the dynamic processes in the extended atmospheres and envelopes of these stars: they can have the form of a spherically symmetric outflow with constant or height dependent velocity, mass infall onto the photosphere, or pulsations. A two-component emission profile is indicative of a more complex, non-spherical wind structure, e.g., a circumstellar disk. An example of such a structure is the profile in the spectrum of BD $48^\circ 1220 = \text{IRAS } 05040+4820$ shown in Fig. 4: observations of this star made with the 6-m telescope resulted in the discovery of its spectral variability

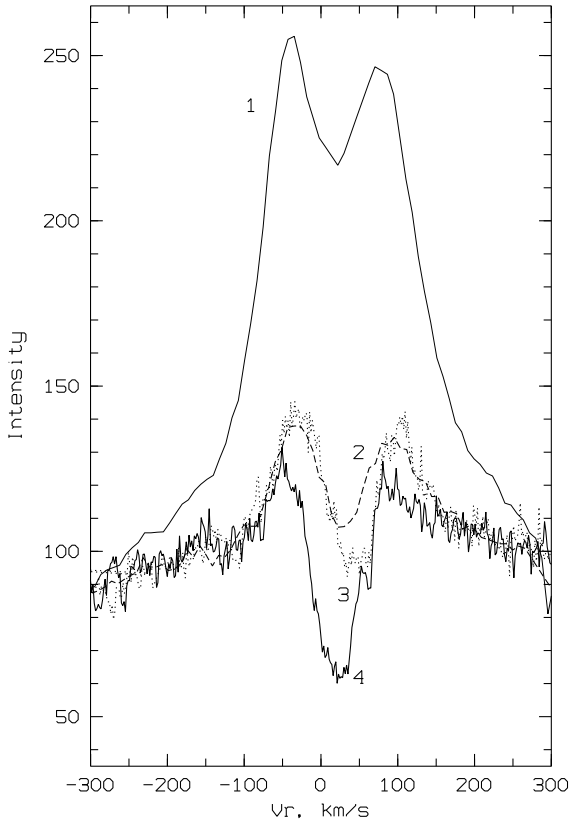


Figure 3. Variability of the absorption and emission profile of the $H\alpha$ line in the spectrum of the optical component of the IR-source IRAS 20508+2011: observations made in 1999 (curve 1), 2000 (curve 2), 2003 (curve 3), and 2004 (curve 4) [49].

and allowed detailed measurements of its chemical composition to be performed and its evolutionary status to be determined [15].

3.2. Molecular Features

Let us now consider the molecular component of the optical spectra of PPNe. The spectra of protoplanetary nebulae with F–K-type supergiant central stars that have carbon-enriched atmospheres show features of carbon-containing molecules C_2 , C_3 , CN, and CH^+ . Kwok et al. [86] report the list of stars with $21\ \mu\text{m}$ emission and C_2 , C_3 , and CN molecular bands in their spectra. Position measurements of molecular features in the spectra indicate that they form in expanding circumstellar envelopes. Bakker et al. (see [68] and references therein) used high-resolution spectra to analyze a large sample of post-AGB stars of this type.

We studied the PPN sample spanning a wide range of spectral types (temperatures) and identified C_2 Swan bands in the spectra of some of these stars (see Table 2). The table also lists the expansion velocities corresponding to the band positions. The most thoroughly studied spectrum is that of the bright star HD 56126 [72]. In the $4010\text{--}8790\ \text{\AA}$ wavelength interval, we performed a detailed identification and measured the positions of the rotational lines of several C_2 vibration bands, identified the CN and CH absorption bands, measured the depths and the corresponding radial velocities of numerous absorptions of neutral atoms and ions as well as interstellar features. Besides the well-known variability of the $H\alpha$ profile, we also found variations of the profiles of a number of Fe II

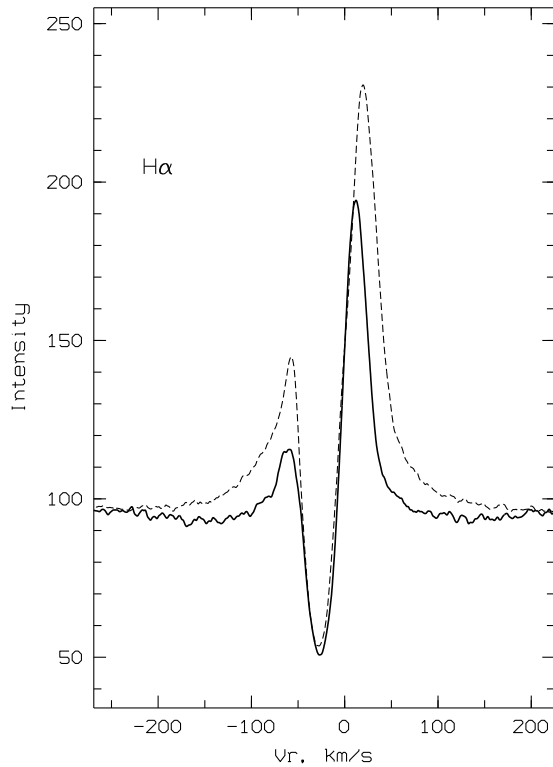


Figure 4. Variability of the absorption and emission profile of the $H\alpha$ line in the spectrum of BD+48°1220, the optical component of the IR source IRAS 05040+4820: March 8, 2004 (the solid line) and January 10, 2004 (the dashed line) [15].

and Ba II lines. The spectra taken in different years show no evidence of emission or variability either in the C_2 molecular bands or in the Na I D-lines. This fact is consistent with a rather simple elliptical shape of the nebula surrounding HD 56126.

It appears that the emission in the Swan bands or Na I D-lines is observed in the spectra of PPNe with bright and conspicuously asymmetric circumstellar nebulae. The results of spectroscopic observations of several PPNe confirm this hypothesis. An analysis of the spectra taken with the 6-m telescope revealed C_2 Swan emission bands of different intensities (relative to the continuum) in the spectra of the central stars of the following sources: IRAS 04296+3429 [13], IRAS 08005–2356 [21], RAFGL 2688 [51], IRAS 22223+4327 [53], and IRAS 23304+6147 [57]. According to HST images [4, 7], these objects have asymmetric (and often bipolar) envelopes; this is also evident from the polarization of their optical emission.

Figure 5 shows fragments of the spectra of a number of objects containing the (0;1) C_2 Swan band. As is evident from the figure, the Swan band is most intense in the spectrum of RAFGL 2688, which belongs to a group of systems whose central parts (the star and the inner regions of the circumstellar envelope) undergo strong absorption in the gas and dust torus (or disk) and where the emission of the central parts is scattered by the dust particles of the bipolar structure. RAFGL 2688 [51] was observed at the 6-m telescope with the spectrograph slit projected onto the northern lobe of the nebula. Because of such an arrangement combined with the strong absorption of the radiation of the central star, the observed spectrum is dominated by the contribution of the emission of the envelope.

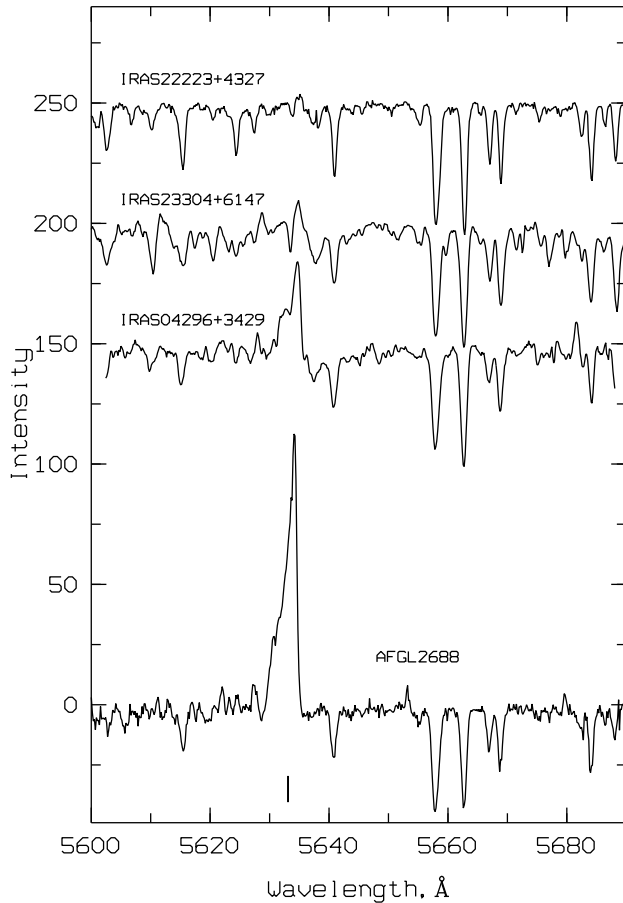


Figure 5. A fragment of the spectra of selected PPNe from Table 2 containing the (0;1) C_2 Swan band.

Klochkova et al. [13] studied the spectrum of IRAS 04296+3429, whose properties are similar to those of RAFGL 2688, and showed that the intensity ratio of different Swan bands corresponds to the resonance fluorescence mechanism.

3.3. Lines of the Na I Resonance Doublet and the Diffuse Bands

In addition to the variable emission components of neutral hydrogen lines and molecular bands, which distinguish the spectra of PPNe from the spectra of normal supergiants, some of them contain features that form in the circumstellar medium. Circumstellar absorption components of the Na I and K I resonance lines are a common feature found in the spectra of PPNe, as expected for objects with circumstellar absorption. Measurements of the positions of circumstellar components are widely used to determine the envelope expansion velocities. This, in particular, applies to HD 161796, HD 101584, and V354 Lac, in whose spectra Bakker et al. [87], Reddy et al. [70], and Kipper [88, 89] found circumstellar components of the Na I D-lines. Klochkova et al. [55] and Klochkova [56] used the spectra obtained with the 6-m telescope to study the Na I D-line profiles and other features in the spectrum of V354 Lac in more detail. The circumstellar absorptions of the Na I D-lines were also identified in the well-studied spectrum of HD 56126 [68, 72, 17]. Much more rarely the circumstellar envelope manifests itself in the form of emission components of the Na I D-lines. Examples include the spectra of V510 Pup, which is the optical counterpart

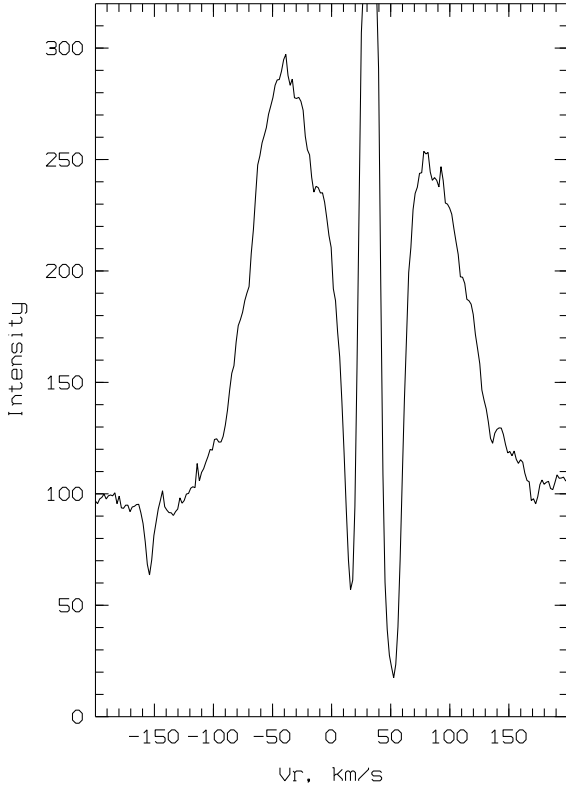


Figure 6. Profile of the Na I D₂ line in the spectrum of QY Sge.

of the IR–source IRAS 08005–2356 [21], bipolar nebula RAFGL 2688 [52], and semiregular variables QY Sge = IRAS 20056+1834 [90, 45] and 89 Her [91].

We now discuss in more detail the spectrum of the yellow supergiant QY Sge, which belongs to a group of objects where the radiation of the central star is obscured by a powerful envelope. Rao et al. [90] identified the main components (an absorption spectrum of a G–type supergiant combined with narrow low excitation emissions and a powerful broad emission in the Na I D lines) in the spectrum of QY Sge and proposed for this object a model with a circumstellar torus and a bipolar mass outflow. According to this model, the central star is completely obscured from the observer, and as a result we see the radiation reflected from the inner wall of the torus. Multiple spectroscopic observations of QY Sge made with the 6–m telescope [45] allowed the kinematic pattern in the atmosphere and envelope of this star to be studied in detail. As is evident from Fig. 6, the complex emission and absorption profile of the Na I D₂ line in the spectrum of QY Sge includes a very broad emission component extending from -170 to $+120$ km s⁻¹. The central part of the broad emission is cut by an absorption feature, which, in turn, is split in two by a narrow emission peak (16 km s⁻¹ at $r=2.5$). The positions of the Na I D emission features remain unchanged, and this fact indicates that the features form in regions that are external to the photosphere of the supergiant.

The pattern of the profile variations of the emission and absorption lines and radial velocities as measured from different profile features is consistent with the model of a toroidal dust envelope that obscures the central source and bipolar cones filled with high-velocity gas. Both in the emission and absorption features of the spectrum, details have been identified that are indicative of spatial and temporal inhomogeneities in the dust and gas components of the object.

A possible relation between the type of the circumstellar nebula and the presence of a Na I D–emission component is difficult to find by analyzing a limited sample of objects. It may be suggested that Na I D–emission is observed in the case where the extended envelope has a complex (for example – bipolar) structure, because the three infrared sources IRAS 08005–2356, RAFGL 2688, and IRAS 20056+1834 with bipolar outflows exhibit Na I D–emission in their spectra. However, contrary to this hypothesis, this emission also appears in the spectrum of 89 Her, where no circumstellar dust envelope has been observed so far [7].

The so-called diffuse interstellar bands (DIBs) have been studied extensively for several decades since their discovery in the 1930s. The origin and chemical identification of these features remain a mystery despite numerous observations and laboratory experiments (see, e.g., the review [92]).

The correlation between the intensity of these bands and interstellar reddening (see [93] and references therein) suggests that dust particles should play a certain part in the formation of DIBs. The similarity of the physical and chemical conditions in the interstellar medium and in circumstellar gas and dust envelopes led the researchers to look for DIB-like features in the spectra of PPNe. As far back as 1993, Bertre and Lequeux [94] identified similar features that formed in circumstellar envelopes in low-resolution spectra of some mass-losing stars. Zacs et al. [95] analyzed high-resolution spectra that we took with the 6–m telescope and suspected that circumstellar components of DIBs may be present in the spectra of HD 179821 and V354 Lac. The medium-resolution spectra of HD 331319 and the optical component of IRAS 23304+6147 taken with the PFES spectrograph [63] also contain strong absorptions whose positions possibly indicate their circumstellar origin [32, 57]. However, the spectroscopic resolution was not high enough to allow more definitive conclusions. Subsequent higher-resolution ($R \geq 60\,000$) observations made with the NES spectrograph mounted on the 6–m telescope revealed several features in the spectrum of V354 Lac that could be identified with circumstellar bands [55]. The mean radial velocity averaged over these features agrees, within the errors, with that determined from the circumstellar component of the profile of the Na I D–lines. Such a coincidence may serve as evidence for the reality of circumstellar DIB analogs.

Luna et al. [96] searched systematically for DIBs in high resolution spectra of a sample of post–AGB stars and concluded that diffuse bands in the spectra of such stars arise in the interstellar medium, whereas the physical conditions in the circumstellar envelopes of these objects do not favor the formation of these features. However, Klochkova [42] recently showed that the optical spectrum of the high latitude post–AGB supergiant V5112 Sgr contains weak absorptions whose positions are indicative of their formation in the circumstellar envelope. The velocities $V_r(\text{DB})$ were measured in the 5780–6613 Å wavelength interval from the positions of reliably identified 5780, 5797, 6196, 6234, and 6379 Å features. The mean $V_r(\text{DB})$ averaged over several spectra and determined with an accuracy better than $\pm 0.5 \text{ km s}^{-1}$ agrees excellently with the velocity determined from the blue component of the Na I D–lines. The resulting agreement leads us to conclude that the weak bands found in the spectrum of V5112 Sgr origin in the circumstellar envelope. Kipper [97] independently came to similar conclusions for the same object based on the spectra of V5112 Sgr taken with a different instrument.

These results mark a new stage in the search for diffuse circumstellar bands.

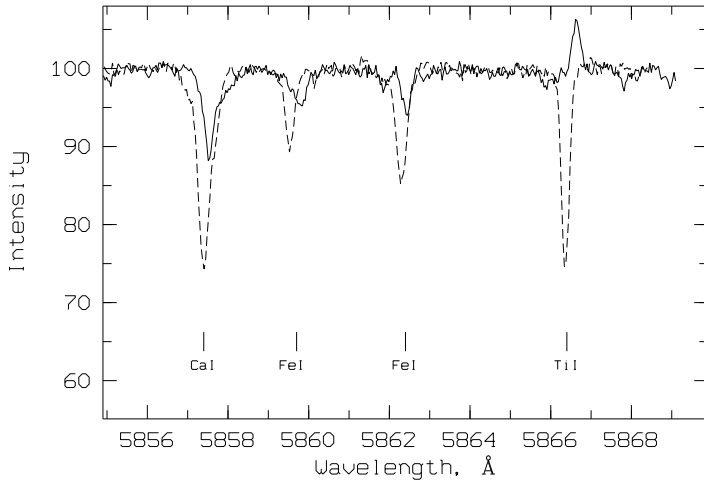


Figure 7. A fragment with the Ti I 5866.40 Å emission in the spectra of LN Hya taken when the stellar atmosphere was in the quiet (April 2, 2010, the dashed line) and excited (June 1, 2010, the solid line) states. Also shown are the identifications of the main spectral features that appear in this fragment.

3.4. Low-Excitation Emissions of Circumstellar Envelopes

The spectra of selected PPNe were found to contain narrow emissions identified with low-excitation metal lines. For example, Bakker et al. [87] thoroughly studied the optical spectrum of the supergiant HD 101584 and found not only symmetric high excitation absorptions and complex P Cyg type profiles but also pure metal emissions, whose positions in the spectrum match the systematic velocity and indicate that the corresponding features origin in the stellar envelope. Kipper [91] also found numerous envelope emissions in the spectrum of 89 Her.

The spectrum of LN Hya taken on June 1, 2010 exhibits a peculiarity previously unknown for this star: weak emissions of neutral atoms (VI, Mn I, Co I, Ni I, Fe I) with intensities amounting to several percent of the continuum level [24]. These emission features were absent in the earlier spectra taken with the 6-m telescope before June 2000. Instead, rather strong absorptions corresponding to the same atomic transitions were observed. Figure 7 shows, by way of an example, a fragment of the spectrum of LN Hya containing one of these emissions—Ti I 5866.40 Å, which appeared on June 1, 2010, when the stellar atmosphere was in an excited state. It follows from the figure that the spectrum contains the Ti I 5866.40 Å emission with an intensity of about 6%, whereas during the period of quiet atmosphere (April 2, 2010) an absorption is observed, whose position matches the radial velocity determined from other undistorted absorptions in the spectrum studied. The intensity of the emissions decreases in the subsequent spectra taken in 2011, and some of these emissions disappear altogether [24]. The atmosphere of the star returned to its normal state, and in 2011 its spectrum, including the H α profile, was practically indistinguishable from the spectrum taken on February 21, 2003. Klochkova and Panchuk [24] could not simultaneously monitor the physical conditions in the stellar atmosphere and in the envelope, and therefore could only suggest that the instability in the upper layers of the atmosphere of LN Hya developed, rapidly amplified, and disappeared during 60 days from April to June 2010.

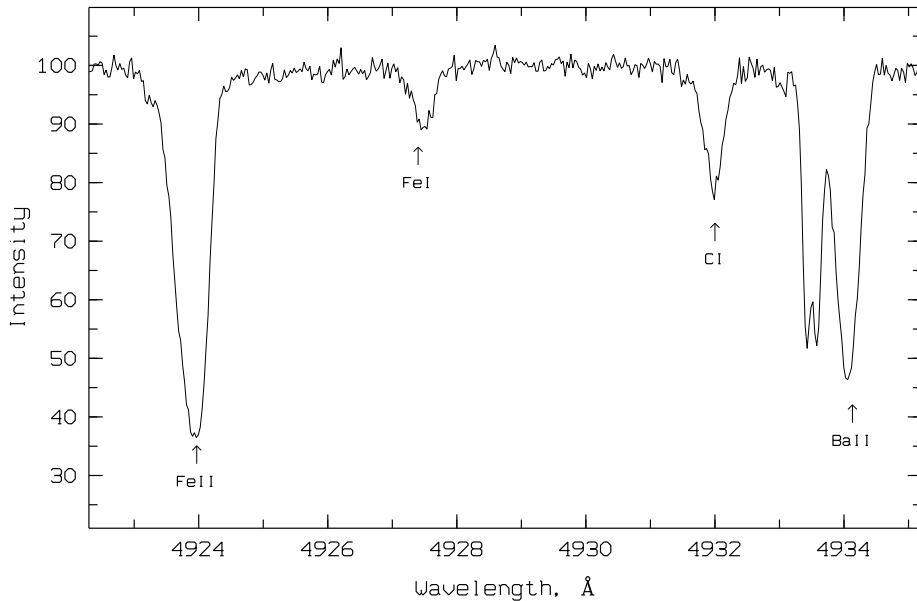


Figure 8. A fragment of the V5112 Sgr spectrum taken on July 7, 2001, containing a split Ba II 4934 Å line.

The constant average velocity of $V_{\text{sys}} = -21.6 \text{ km s}^{-1}$, measured from weak symmetric emissions of neutral atoms (VI, Mn I, Co I, Ni I, Fe I), can be adopted as the systemic velocity for LN Hya. The same velocity value was measured from the emission component of the Na I D lines, whose position also does not change with time.

Note that the stars mentioned in this section (89 Her, LN Hya, and HD 101584) constitute a group of related objects in terms of chemical composition: they have low metallicity and are underabundant in heavy metals.

3.5. Peculiar Profiles of Strong Absorptions

The systematic monitoring of PPN candidates and related objects with envelopes performed with a high spectral resolution produced a new result—the discovery of peculiar profiles of the strongest absorptions in the spectra of selected objects: HD 56126 [72], V354 Lac [54], V448 Lac [53], and V5112 Sgr [42]. Let us illustrate this effect using the example of the spectrum of the supergiant V5112 Sgr, where it is most pronounced.

In the spectra of V5112 Sgr, taken in a wide wavelength interval, we found in addition to the variable H α profile other, previously unknown peculiarities. The strongest absorptions have anomalous profiles: they are either asymmetric with extended blue wings or split into individual components. Figure 8 shows a fragment of the spectrum of V5112 Sgr taken on July 7, 2001 with a split Ba II 4934 Å line. The different widths of the components are immediately apparent: the red component is about twice broader than the blue components, which are offset substantially relative to the systemic velocity. This difference between the component widths indicates that the red and blue components form under different physical conditions. At the same time, the profiles of strong absorptions of iron-group metals in the spectrum of this star are neither asymmetric nor split, as is immediately apparent from the same Fig. 8, where we see a very strong but unsplit Fe II 4924 Å line.

A comparison of the line profiles in the spectra of V5112 Sgr taken during different nights reveals substantial variability of the profile shapes and of the positions of the

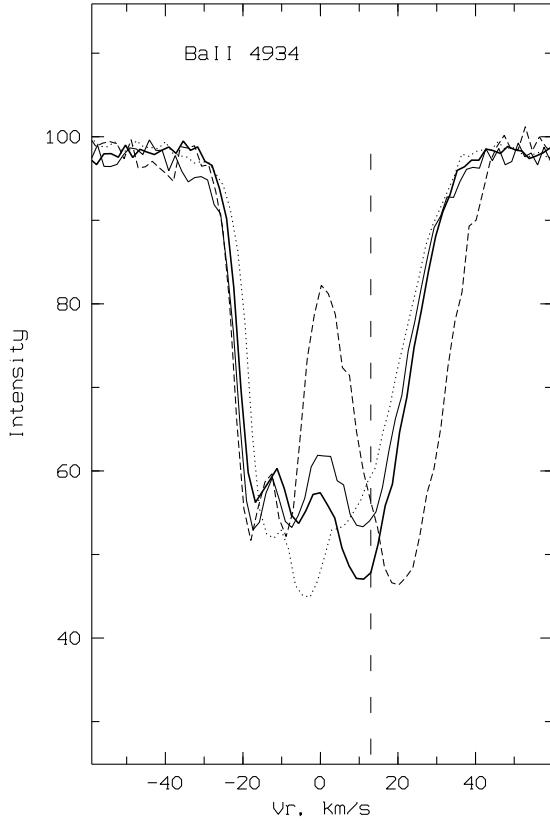


Figure 9. Variability of the Ba II 4934 Å line profile in the spectra of V5112 Sgr taken in different years: August 2, 2012 (the thin solid line); June 13, 2011 (the solid bold line); August 14, 2006 (the dotted line); July 7, 2001 (the dashed line) [42].

components of the split lines. To illustrate the variability effect, we show in Fig. 9 the Ba II 4934 Å line profile, which is most asymmetric and most variable. It follows from this figure that the position of the photospheric (red) component of the complex profile is variable, whereas the blue components, which, as shown in [42], form in the envelope, are stable.

The semiregular variable V354 Lac is the closest analog to V5112 Sgr among the objects listed in Table 2 in terms of the structure of the envelope and spectral peculiarities. The spectroscopic monitoring of this star [55] carried out at the SAO 6-m telescope with a resolution of $R = 60\,000$ revealed the splitting of the strongest absorptions with the low-level excitation potential of $\chi_{\text{low}} \leq 1$ eV. An analysis of the kinematic pattern showed that the blue component of the split line forms in the powerful gas and dust envelope of V354 Lac. This splitting shows up most conspicuously in the profile of the strong Ba II 6141 Å line. The shift of the blue component of the Ba II line coincides with that of the circumstellar component of Na I D lines, which forms in the same layers as the circumstellar C₂ Swan bands. This coincidence indicates that the complex profile of the Ba II 6141 Å line contains, in addition to the atmospheric component, a component that forms in the circumstellar envelope. Such splitting (or the profile asymmetry due to the more shallow slope of the blue wing) is also observed for other Ba II ($\lambda\lambda$ 4554, 5853, 6496 Å) lines as well as for the strong Y II 5402 Å, La II 6390 Å, and Nd II 5234, 5293 Å lines. The lines of these ions in the spectrum of V354 Lac are enhanced to the extent that their intensities are comparable to those of neutral-hydrogen lines. For example, the

equivalent width of the Ba II 6141 Å line reaches $W_\lambda \approx 1$ Å, and that of H β reaches $W_\lambda \approx 2.5$ Å.

The difference between the peculiarity types of the profiles of two pairs of stars—V5112 Sgr and V354 Lac with split profiles of the strongest absorptions of selected elements, and HD 56126 and V448 Lac with asymmetric but unsplit profiles—suggests that the morphology of the circumstellar envelope may be the factor that causes the peculiarity and variability of the profiles of the strongest lines. As is evident from Table 2, the two stars V5112 Sgr and V354 Lac with split absorptions have bipolar envelopes, whereas the absorptions are unsplit in the spectra of HD 56126 and V448 Lac and the envelopes of these stars have a less defined structure.

This hypothesis is further corroborated by the three-component structure of the strong absorption profiles observed in the spectrum of V5112 Sgr, where CO observations show both the slow ($V_{\text{exp}} = 10 \text{ km s}^{-1}$) and the fast ($30\text{--}40 \text{ km s}^{-1}$) expansion [98]. The profiles of the split lines include a photospheric component and two envelope components, one of which, like in the case of the CO profile, arises in the envelope that formed at the AGB-stage and expands at a velocity of $V_{\text{exp}}(2) \approx 20 \text{ km s}^{-1}$, and the other one arises in the envelope that moves at a velocity of $V_{\text{exp}}(1) \approx 30 \text{ km s}^{-1}$ and formed later. Similar peculiarities of the profiles of low excitation absorptions, the variability of the optical spectra, and the Swan emission bands were also found for two other objects from Table 2: IRAS 22223+4327 [53] and IRAS 23304+6147 [99].

The splitting of strong low excitation absorptions is observed in the spectra of luminous stars of various types. One of the well-known cases is the complex kinematic pattern in the outflowing atmosphere of the yellow supergiant ρ Cas. Current results of spectroscopic monitoring are reported in [100, 58]. The splitting of absorptions at certain light-curve phases in the spectra of W Vir type variables (see Sanford's results [101] for W Vir), classical Cepheids [102], RV Tau type variables [103], and Miras has been known since the mid-20th century. Kovtykh et al. [104] studied the variation of the profiles of emission-containing lines in the spectrum of W Vir with pulsation phase and proposed a scheme based on two shocks localized in the atmosphere and envelope. A hydrodynamic model of the extended atmosphere of this star has been developed to explain these variations. Advanced spectroscopy tools have also made it possible to detect the doubling of metal lines in the spectra of the short-period pulsating star RR Lyr [105].

Sanford [101] attributed the splitting of absorptions and the presence of strong emission in hydrogen and helium lines in the spectra of pulsating stars to shock propagation (the Schwartzschild mechanism [106]). However, the efficiency of the Schwartzschild mechanism in the case of PPNe is open to question, because atmospheric pulsations in the atmospheres of these objects have low amplitudes, $\Delta V_r \approx 1 \div 3 \text{ km s}^{-1}$ [72, 53, 55, 56, 80]. It therefore remains unclear how the shocks, whose generation requires higher pulsation amplitudes ($\Delta V_r \geq 5 \div 10 \text{ km s}^{-1}$ [107]), may develop.

4. DISCUSSION OF THE RESULTS

The primary conclusion of the analysis of the properties of the supergiants with infrared excess studied so far is that the available sample of these objects is inhomogeneous. These objects are found to exhibit a great variety of peculiarities in the optical spectra of their central stars, the chemical composition of their atmospheres and envelopes, and the morphology and kinematic state of their circumstellar envelopes. We should point out, in particular, that supergiants with infrared excess include RV Tau type variables. These variable stars with near-infrared excesses undergo the post-AGB evolutionary stage, and

most of them are binaries [81]. They owe their peculiar chemical composition to the high efficiency of selective separation processes [108].

One of the important results of the study is the formation of a subsample of PPNe with atmospheres enriched in carbon and heavy metals synthesized during the AGB evolution. It follows from Table 2 that all these PPNe are also distinctive in that their spectra contain the $21\ \mu\text{m}$ emission, which arises in the circumstellar medium. Attempts to find an interconnection between the morphology of the envelope and the peculiarities of the chemical composition of the central star revealed no strict correlation. It may nevertheless be concluded that objects with enriched atmospheres (IRAS 02229+6208, 04296+3429, 19500–1709, and 23304+6147) mostly have structured (bipolar) envelopes. However, objects with enriched atmospheres also include IRAS 05113+1347, whose envelope even the HST failed to resolve, as well as IRAS 05341+0852 and 07134+1005 with envelopes in the form of elongated haloes. One should also pay attention to IRAS 19475+3119, which has a structured envelope, whereas the atmosphere of its central star HD 331319 is not enriched in either carbon or heavy metals. However, helium lines were found and reliably measured in the spectrum of HD 331319. The presence of these lines in the spectrum of a star with $T_{\text{eff}} = 7200\ \text{K}$ results in a significant helium overabundance in its atmosphere [32], which can be viewed as a manifestation of helium synthesis during prior evolution. Helium overabundances were earlier found in HD 44179 = IRAS 06176–1036 [109] and V5112 Sgr [110].

The $\text{H}\alpha$ lines in the spectra of PPNe usually have complex profiles (a combination of absorption and emission components) and are variable in time. It is evident that the surface-most atmospheric layers, which are susceptible to stellar-wind influence, and the outflowing circumstellar envelope effect the formation of neutral hydrogen line profiles. We do not model these profiles in this paper, that is the aim of a separate study. Here we only emphasize the importance of spectroscopic monitoring in solving this problem. A good example is the sharp change of the $\text{H}\alpha$ profile in the spectrum of V5112 Sgr which happened at the turn of the century: in 1996 the line had the form of an inverse P Cyg type profile, and in the 2000s the profile already contained two emission components [42]. Note that this change of the $\text{H}\alpha$ profile type, which has been recorded in the spectra taken with the 6-m telescope, occurred simultaneously with a significant change of the photometric properties of the object as detected by Hrivnak et al. [79] during their long-term monitoring.

The optical spectra of PPNe with enriched atmospheres are often found to exhibit spectral features of carbon-containing molecules. In particular, the wavelength interval accessible to our instruments contains Swan C_2 bands. The data provided in Table 2 leads us to conclude that Swan bands in the spectra of PPNe are observed over a rather broad range of effective temperatures of the central star, starting from the late G-type stars ($T_{\text{eff}} \approx 5000\ \text{K}$). The spectra of hotter objects with $T_{\text{eff}} \geq 7500\ \text{K}$ contain no molecular features because the molecules are destroyed by the radiation of the hot star. The hottest star with Swan bands in our list is the source IRAS 08005–2356, whose central star has a temperature of $T_{\text{eff}} = 7300\ \text{K}$. The presence of Swan bands in the cases where the central star is rather hot can most likely be explained by the presence of two envelopes made of cool and hot dust. Bakker et al. [68] determined the dust temperature in the envelopes of IRAS 08005–2356 to be $T_{\text{dust}} \leq 150\ \text{K}$ and $T_{\text{dust}} \geq 1200\ \text{K}$. According to the data of the above authors, Swan C_2 bands are observed in the spectra of objects with cool dust envelopes ($T_{\text{dust}} \leq 300\ \text{K}$).

Note yet another peculiarity in the appearance of Swan bands in the spectra of the objects studied. It can be seen from Table 2 that the data on the presence or absence and the type of circumstellar Swan C_2 bands differ for different observations of the same object.

A comparison of the data on the presence of Swan bands according to Table 3 in [68] with our data listed in Table 2 leads us to conclude that discrepant results are obtained for common objects. For example, Bakker et al. [68] point out the 5635 Å absorption band in the spectrum of RAFGL 2688, where a strong emission band at 5635 Å was found, according to the observations made with the 6-m telescope (Fig. 5). In their recent study of the spectrum of RAFGL 2688, Ishigaki et al. [75] point out a very strong emission in the molecular bands. The spectra of IRAS 08005–2356 taken with the 6-m telescope [21] show strong Swan absorption bands, whereas Bakker et al. [68] report uncertain results for this object. Bakker et al. [68] report Swan absorption bands for the IRAS 22223+4327 source with a powerful structured envelope, whereas more recent observations of this object made with the 6-m telescope show emission bands [53].

These discrepancies may be due both to temporal variations of the physical conditions in the circumstellar envelopes of PPNe (caused by the deviation from symmetry and sphericity) and different observing conditions for extended structures when studied with different telescopes: the differences in the spectrograph slit orientation and seeing may result in different flux contributions from the central star and the envelope. Note, for example, a significant difference between the measured intensities of the emission component of the Na I D-lines reported by Klochkova et al. [51] and Ishigaki et al. [75]. The large difference between the measured fluxes is due not only to the factor-of-two difference in the spectral resolution of the data reported in [51] and [75] but also to physical factors. It is evident that there may be objects with such dust disk orientation that the central star is not obscured from the observer, and its flux is not reduced by several factors of ten. In this case both the torus (or disk) and the scattering lobes are difficult to detect optically because of their proximity to the bright star, and no bipolar nebula is observed. The spectrum of the central star in a system with such orientation may show no molecular emission bands, because the emission in these bands is “drowned” in the radiation of the photosphere. The difference between the morphologies of “extended halo” and “bipolar” type nebulae may be purely visual, because the observed shape depends strongly on the inclination of the structure to the line of sight and the angular resolution [5]. For example, according to the data of Nakashima et al. [111], the extended envelope of HD 56126 shows no clear structure in the form of jets, cavities, etc.

The most recent result in the optical spectroscopy of PPNe is the discovery of the heavy-metal enrichment of the circumstellar envelope of the V5112 Sgr supergiant [42]. The splitting of the profiles of the strongest heavy-metal absorptions in the spectrum of this star with a complex bipolar envelope suggests that the process of the formation of a structured circumstellar envelope may contribute to the enrichment of this envelope by products of stellar nucleosynthesis. The profiles of the split lines contain a photospheric and two envelope components, one of which, like in the case of the CO-profile, arises in the envelope that formed at the AGB-stage and expands at a velocity of $V_{\text{exp}}(2) \approx 20 \text{ km s}^{-1}$, and the other one—in the envelope that formed later and expands at a velocity of $V_{\text{exp}}(1) \approx 30 \text{ km s}^{-1}$. The circumstellar components of strong heavy-metal absorptions have also been conclusively identified in the spectrum of V354 Lac [55]. Note that it is for these two related objects, V5112 Sgr 42 and V354 Lac [55], that we made the conclusion about the presence of circumstellar DIB-like absorptions in their spectra.

The structure of the circumstellar nebula of V354 Lac may be more complex than it appears in the HST observations (see Table 2). Polarimetric observations by Gledhill et al. [112] indicate the presence of a ring structure embedded in an extended nebula. Nakashima et al. [113] point out that the axes of the optical and infrared images of the nebula are almost perpendicular to each other. Based on the kinematic pattern of

the nebula as determined from the mapping of the CO–emission, Nakashima et al. [113] concluded that the structure of the nebula includes not only a torus and a spherical component but also another element (possibly a jet).

The asymmetry (and, in particular, bipolarity) of the structure of selected PPNe was found in several types of observations. Fundamentally important information about the envelope morphology and dust grain properties in circumstellar envelopes can be obtained from spectropolarimetric observations. It follows from the observations of Bieging et al. [9] that more than 70% of AGB and post–AGB stars have intrinsic polarization. The high linear polarization degree of their radiation is in itself indicative of the asymmetry of the envelope. Examples include objects with bipolar envelopes, such as RAFGL 618 [114] and RAFGL 2688 [52]. The linear polarization spectrum of RAFGL 2688 taken with the 6–m telescope with a good spectral resolution ($R=15\,000$) in the 5000–6600 Å wavelength interval allowed the features of photospheric and circumstellar origin to be separated for the first time. Klochkova et al. [52], in particular, established that emission in the Swan system lines forms in the envelope and that the corresponding transitions are excited by resonance fluorescence [52].

Currently, no consensus has been reached concerning the development of deviations from spherical symmetry in PPNe. Ueta et al. [4, 7] analyzed high spatial resolution optical images of a sample of PPNe taken by the Hubble Space Telescope and concluded that the optical depth of the circumstellar matter is the crucial factor that determines the formation of a particular morphology of stellar envelopes. The dense and often spherical [115] envelope that formed during the AGB–stage is believed to expand slowly, whereas the rapidly expanding feature is the axisymmetric part of the envelope that formed later at the post–AGB stage. The sequence of these processes results in the development of an optical depth gradient in the direction from the equator to the polar axis of the system. The presence of a companion and/or a magnetic field in the system may also prove to be the physical factor that causes the loss of the spherical symmetry of the stellar envelope during the short evolutionary interval between the AGB and post–AGB stages (see [116, 117] and references therein). In their recent paper Koning et al. [118] proposed a simple PPN model based on a pair of evacuated cavities inside a dense spherical halo. The above authors demonstrated that all the morphological features observed in real bipolar PPNe can be reproduced by varying the available parameters (mass density inside the cavity, its size and orientation) of this model.

So far, the discovery of the heavy-metal enrichment of the circumstellar envelopes of the supergiants V5112 Sgr and V354 Lac remains a unique result. It may be followed up by high-resolution spectroscopy of closely related objects. We believe the most promising objects to be IRAS 04296+3429 and 23304+6147. It follows from Table 2 that the atmospheres of the faint central stars of these sources are enriched in heavy metals, and their circumstellar envelopes have a complex structure.

5. MAIN CONCLUSIONS

We used the results of high spectral resolution observations made with the 6–m telescope of the Special Astrophysical Observatory to analyze the peculiarities of the optical spectra of a sample of post–AGB stars with atmospheres enriched in carbon and heavy s–process metals and with carbon-enriched circumstellar envelopes.

We showed that the peculiarities of the line profiles (the presence of an emission component in the lines of the Na I D–doublet, the type of the molecular features, the asymmetry and splitting of the profiles of strong absorptions with a low excitation potential of the

low level) are associated with the kinematic and chemical properties of the circumstellar envelope and the type of its morphology. In particular, the variability of the observed profiles of H α absorption and emission lines and those of metal lines as well as the change of the type (absorption/emission) of C₂ Swan bands observed in some objects are associated with the changes in the structure of the circumstellar envelope.

The type of the H α profile (pure absorption, pure emission, P Cyg or inverse P Cyg, with two emission components in the wings) is unrelated to the chemical composition of the atmosphere of the central star. The main factors that influence the type of the H α profile and its variability are the mass loss rate, stellar wind velocity, kinematics and optical depth of the envelope.

The splitting of the profiles of the strongest heavy-metal absorptions in the spectra of the V5112 Sgr and V354 Lac supergiants found as a result of our observations suggests that the formation of a structured circumstellar envelope is accompanied by the enrichment of this envelope with the products of stellar nucleosynthesis. Note that it is in the spectra of these two related objects, V5112 Sgr and V354 Lac, that we found DIB-like envelope absorptions.

Attempts to find a relation between the peculiarities of the optical spectrum and the morphology of the circumstellar medium are complicated by the fact that the observed structure of the envelope depends strongly on the inclination of the symmetry axis to the line of sight and on the angular resolution of the spectroscopic and direct-imaging instruments.

Acknowledgments

I am deeply grateful to all the coauthors who took part in carrying out the program of spectroscopic observations of supergiants with IR excesses at the SAO 6-m telescope. This work was supported by the Russian Foundation for Basic Research (project No. Envelopes14-02-00291 a). This research has made use of the SIMBAD database, operated at CDS, Strasbourg, France, and NASA Astrophysics Data System. Observations at the 6-m telescope of the Special Astrophysical Observatory are carried out with the financial support of the Ministry of Education and Science of the Russian Federation (contracts No. 14.518.11.7070 and 16.518.11.7073).

References

1. M. Busso, R. Gallino, and G. J. Wasserburg, *Ann. Rev. Astron. Astrophys.* **37**, 239 (1999).
2. F. Herwig, *Ann. Rev. Astron. Astrophys.* **43**, 435 (2005).
3. B. Gustafsson and N. Ryde, *IAU Symp.*, No. 210, 481 (2000).
4. T. Ueta, M. Meixner, and M. Bobrowsky, *Astrophys. J.* **528**, 861 (2000).
5. R. Sahai, M. Morris, C. Sánchez Contreras, and M. Claussen, *Astron. J.* **134**, 2200 (2007).
6. N. L. J. Cox, D. A. García-Hernández, P. García-Lario, and A. Manchado, *Astron. J.* **141**, 111 (2011).
7. N. Siódmiak, M. Meixner, T. Ueta, et al., *Astrophys. J.* **677**, 382 (2008).
8. E. Lagadec, T. Verhoelst, D. Mékarnia, et al., *Mon. Not. R. Astron. Soc.* **417**, 32 (2011).
9. J. H. Bieging, G. D. Schmidt, P. S. Smith, and B. D. Oppenheimer, *Astrophys. J.* **639**, 1053 (2006).
10. A. S. Miroshnichenko, E. L. Chentsov, V. G. Klochkova, et al., *Astrophys. J.* **700**, 209 (2009).
11. V. G. Klochkova, M. V. Yushkin, A. S. Miroshnichenko, et al., *Astron and Astrophys.* **392**, 143 (2002).
12. T. Kipper and V. G. Klochkova, *Baltic Astronomy* **14**, 215, (2005).
13. V. G. Klochkova, R. Szczerba, V. E. Panchuk, and K. Volk, *Astron and Astrophys.* **345**, 905 (1999).
14. V. G. Klochkova, E. L. Chentsov, V. E. Panchuk, and M. V. Yushkin, *IBVS*, No. 5584 (2004).
15. V. G. Klochkova, E. L. Chentsov, N. S. Tavalzhanskaya, and V. E. Panchuk, *Astron. Rep.* **51**, 642 (2007).
16. V. G. Klochkova and E. L. Chentsov, *Astrophys. Bull.* **63**, 272 (2008).
17. V. G. Klochkova and E. L. Chentsov, *Astron. Rep.* **51**, 994 (2007).
18. V. G. Klochkova, *Mon. Not. R. Astron. Soc.* **272**, 710 (1995).
19. V. P. Arkhipova, V. G. Klochkova, E. L. Chentsov, et al., *Astron. Lett.* **32**, 661 (2006)
20. V. G. Klochkova and V. E. Panchuk, *Astrophys. Bull.* **41**, 5 (1996).
21. V. G. Klochkova and E. L. Chentsov, *Astron. Rep.* **48**, 301 (2004).
22. V. G. Klochkova and T. V. Mishenina, *Astrophys. Bull.* **44**, 83 (1998).
23. V. G. Klochkova and V. E. Panchuk, *Astron. Lett.* **14**, 395 (1988).
24. V. G. Klochkova and V. E. Panchuk, *Astron. Rep.* **56**, 104 (2012).
25. T. Kipper and V. G. Klochkova, *Baltic Astronomy* **15**, 531 (2006).
26. T. Kipper and V. G. Klochkova, *Baltic Astronomy* **15**, 521 (2006).
27. V. G. Klochkova and V. E. Panchuk, *Sov. Astron. Lett.* **15**, 264 (1989).

28. V. G. Klochkova, V. E. Panchuk, and E. L. Chentsov, *Astron and Astrophys.* **323**, 789 (1997).
29. V. G. Klochkova and N. N. Samus, *Astron and Astrophys.* **378**, 455 (2001).
30. V. G. Klochkova, V. E. Panchuk, N. S. Tavganskaya, and V. V. Kovtyukh, *Astron. Let.* **29**, 748 (2003).
31. T. Kipper and V. G. Klochkova, *Astron and Astrophys.* **324**, L65 (1997).
32. V. G. Klochkova, V. E. Panchuk, and N. S. Tavganskaya, *Astron. Let.* **28**, 49 (2002).
33. V. G. Klochkova and V. E. Panchuk, *Astron. Let.* **14**, 933 (1988).
34. V. P. Arkhipova, V. G. Klochkova, and G. V. Sokol, *Astron. Let.* **27**, 99 (2001).
35. T. Sahin, D. L. Lambert, V. G. Klochkova, and N. S. Tavganskaya, *Mon. Not. R. Astron. Soc.* **410**, 612 (2011).
36. V. G. Klochkova, G. Zhao, V. E. Panchuk, and N. S. Tavganskaya, *Astron. Rep.* **45**, 553 (2001).
37. T. Kipper and V. G. Klochkova, *Baltic Astronomy* **22**, 77, (2013).
38. L. Zacs, V. G. Klochkova, V. E. Panchuk, and R. Spelmanis, *Mon. Not. R. Astron. Soc.* **282**, 1171 (1996).
39. V. G. Klochkova, E. L. Chentsov, and V. E. Panchuk, *Mon. Not. R. Astron. Soc.* **292**, 19 (1997).
40. V. G. Klochkova, M. V. Yushkin, E. L. Chentsov, and V. E. Panchuk, *Astron. Rep.* **46**, 139 (2002).
41. H. van Winckel and M. Reyniers, *Astron and Astrophys.* **354**, 135 (2000).
42. V. G. Klochkova, *Astron. Let.* **39**, 765 (2013).
43. V. G. Klochkova and T. Kipper, *Baltic Astronomy* **15**, 395, (2006).
44. V. G. Klochkova, T. V. Mishenina, and V. E. Panchuk, *Astron. Let.* **26**, 398 (2000).
45. V. G. Klochkova, V. E. Panchuk, E. L. Chentsov, and M. V. Yushkin, *Astrophys. Bull.* **62**, 217 (2007).
46. T. Kipper, M. Kipper, and V.G. Klochkova, *Astron and Astrophys.* **297**, L33, (1995).
47. T. Kipper and V. Klochkova, *Baltic Astronomy* **10**, 393, (2001).
48. V. P. Arkhipova, N. P. Ikonnikova, R. I. Noskova, et al., *Astron. Let.* **27**, 719 (2001).
49. V. G. Klochkova, V. E. Panchuk, N. S. Tavganskaya, and G. Zhao, *Astron. Rep.* **50**, 232 (2006).
50. V. G. Klochkova, E. L. Chentsov, and V. E. Panchuk, *Astrophys. Bull.* **63**, 112 (2008).
51. V. G. Klochkova, R. Szczerba, and V. E. Panchuk, *Astron. Let.* **26**, 439 (2000).
52. V. G. Klochkova, V. E. Panchuk, M. V. Yushkin, and A. S. Miroshnichenko, *Astron. Rep.* **48**, 288 (2004).
53. V. G. Klochkova, V. E. Panchuk, and N. S. Tavganskaya, *Astron. Rep.* **54**, 234 (2010).

54. L. Zacs, V. G. Klochkova, and V. E. Panchuk, *Mon. Not. R. Astron. Soc.* **275**, 764 (1995).
55. V. G. Klochkova, V. E. Panchuk, and N. S. Tavganskaya, *Astrophys. Bull.* **64**, 155 (2009).
56. V. G. Klochkova, *Astron. Let.* **35**, 457 (2009).
57. V. G. Klochkova, R. Szczerba, and V. E. Panchuk, *Astron. Let.* **26**, 88 (2000).
58. V. G. Klochkova, V. E. Panchuk, N. S. Tavganskaya, and I. A. Usenko, *Astron. Rep.* **58**, 101 (2014).
59. V. Panchuk, V. Klochkova, M. Yushkin, and I. Najdenov, in *Proc. Joint Discussion No. 4 during the IAU General Assembly 2006, UV Astronomy: Stars from Birth to Death*, Ed. by A. I. Gómez de Castro and M. A. Barstow (Editorial Complutense, Madrid, 2007), p. 179.
60. V. Panchuk, V. Klochkova, M. Yushkin, and I. Najdenov, *J. Optical Technology* **76**, 87 (2009).
61. V. Panchuk, V. Klochkova, I. Najdenov, et al., Preprint No. 139 (Special Astrophysical Observatory, Russian Academy of Sciences, 1999).
62. V. Panchuk, M. Yushkin, and I. Najdenov, Preprint No. 179 (Special Astrophysical Observatory, Russian Academy of Sciences, 2003).
63. V. E. Panchuk, J. D. Najdenov, V. G. Klochkova, et al., *Astrophys. Bull.* **44**, 127 (1998).
64. M. Yushkin and V. Klochkova, Preprint No. 206 (Special Astrophysical Observatory, Russian Academy of Sciences, 2005).
65. V. G. Klochkova, *Astrophys. Bull.* **67**, 385 (2012).
66. B. E. Reddy, E. J. Bakker, and B. J. Hrivnak, *Astrophys. J.* **524**, 831 (1999).
67. B. J. Hrivnak and J. H. Biegging, *Astrophys. J.* **624**, 331 (2005).
68. E. J. Bakker, E. F. van Dishoeck, L. B. F. M. Waters, and T. Schoenmaker, *Astron and Astrophys.* **323**, 469 (1997).
69. C. Loup, T. Forveille, A. Omont, and J. P. Paul, *Astron and Astrophys. Suppl.* **99**, 291 (1993).
70. B. E. Reddy, D. L. Lambert, G. Gonzalez, and D. Yong, *Astrophys. J.* **564**, 482 (2002).
71. B. E. Reddy, M. Parthasarathy, G. Gonzalez, and E. J. Bakker, *Astron and Astrophys.* **328**, 331 (1997).
72. V. G. Klochkova, E. L. Chentsov, N. S. Tavganskaya, and M. V. Shapovalov, *Astrophys. Bull.* **62**, 162 (2007).
73. J. Y. Hu, P. te Lintel Hekkert, S. Slijkhuis, et al., *Astron and Astrophys. Suppl.* **103**, 301 (1994).
74. A. Omont, C. Loup, T. Forveille, et al., *Astron and Astrophys.* **267**, 515 (1993).
75. M. N. Ishigaki, M. Parthasarathy, B. E. Reddy, et al., *Mon. Not. R. Astron. Soc.* **425**, 997 (2012).
76. B. J. Hrivnak, K. Volk, and S. Kwok, *Astrophys. J.* **694**, 1147 (2009).
77. S. Kwok, *Ann. Rev. Astron. Astrophys.* **31**, 63 (1993).

78. A. Li, J. M. Liu, and B. W. Jiang, *Astrophys. J.* **777**, 111 (2013).
79. B. J. Hrivnak, W. Lu, R. E. Maupin, and B. D. Spitzbart, *Astrophys. J.* **709**, 1042 (2010).
80. B. J. Hrivnak, W. Lu, K. L. Wefel, et al., *Astrophys. J.* **734**, 25 (2011).
81. H. van Winckel, *Baltic Astronomy*, **16**, 112 (2007).
82. N. R. Trams, L. B. F. M. Waters, C. Waelkens, et al., *Astron and Astrophys.* **218**, L1 (1989).
83. C. Sánchez Contreras, R. Sahai, A. Gil de Paz, and R. Goodrich, *Astrophys. J. Suppl.* **179**, 166 (2008).
84. R. D. Oudmaijer and E. J. Bakker, *Mon. Not. R. Astron. Soc.* **271**, 615 (1994).
85. V. G. Klochkova, *Astrophys. Bull.* **44**, 5 (1997).
86. S. Kwok, K. Volk, and B. J. Hrivnak, *IAU Symp.*, No. 191, 297 (1999).
87. E. J. Bakker, H. J. G. L. M. Lamers, L. B. F. M. Waters, et al., *Astron and Astrophys.* **307**, 869 (1996).
88. T. Kipper, *Baltic Astronomy* **14**, 223 (2005).
89. T. Kipper, *Baltic Astronomy* **16**, 191 (2007).
90. N. Kameswara Rao, A. Goswami, and D. L. Lambert, *Mon. Not. R. Astron. Soc.* **334**, 129 (2002).
91. T. Kipper, *Baltic Astronomy* **20**, 65 (2011).
92. P. J. Sarre, *J. Molecular Spectroscopy* **238** (1), 1 (2006).
93. J. Kos and T. Zwitter, *Astrophys. J.* **774**, 72 (2013).
94. T. Le. Bertre and J. Lequeux, *Astron and Astrophys.* **274**, 909 (1993).
95. L. Zacs, M. R. Schmidt, and R. Szczerba, *Mon. Not. R. Astron. Soc.* **306**, 903 (1999).
96. R. Luna, N. L. J. Cox, M.A. Satorre, et al., *Astron and Astrophys.* **480**, 133 (2008).
97. T. Kipper, *Baltic Astronomy* **22**, 297 (2013).
98. V. Bujarrabal, J. Alcolea, and P. Planesas, *Astron and Astrophys.* **257**, 701 (1992).
99. V. G. Klochkova and N. S. Tavolgenskaya, *Astron. Let.* (in press).
100. N. Gorlova, A. Lobel, A.J. Burgasser, et al., *Astrophys. J.* **651**, 1130 (2006).
101. R. F. Sanford, *Astrophys. J.* **116**, 331 (1952).
102. R. P. Kraft, *Publ. Astron. Soc. Pasif.* **68** No. 401, 137 (1956).
103. G. W. Preston, *Astrophys. J.* **136**, 866 (1962).
104. V. V. Kovtyukh, G. Wallerstein, S. M. Andrievsky, et al., *Astron and Astrophys.* **526**, A116 (2011).
105. M. Chadid and D. Gillet, *Astron and Astrophys.* **308**, 481 (1996).
106. M. Schwarzschild, *Harvard College Observ. Circ.*, No. 429, 1 (1938).

107. N. Kameswara Rao, *Bull. Astron. Soc. India*, **33**, 159 (2005).
108. S. Giridhar, D. L. Lambert, B. E. Reddy, et al., *Astrophys. J.* **627**, 432 (2005).
109. C. Waelkens, H. van Winckel, N. R. Trams, and L. B. F. M. Waters, *Astron and Astrophys.* **256** L15 (1992).
110. H. van Winckel, C. Waelkens, and R. D. Oudmaijer, *Astron and Astrophys.* **312**, 553 (1996).
111. J. Nakashima, N. Koning, S. Kwok, and Y. Zhang, *Astrophys. J.* **692**, 402 (2009).
112. T. M. Gledhill, A. Chrysostomou, J. H Hough, and J. A. Yates, *Mon. Not. R. Astron. Soc.* **322**, 321 (2001).
113. J. Nakashima, N. Koning, N. H. Volgenau, et al., *Astrophys. J.* **759**, 61 (2012).
114. G. D. Schmidt and M. Cohen, *Astrophys. J.* **246**, 444 (1981).
115. A. Castro-Carrizo, G. Quintana-Lacaci, R. Neri, et al., *Astron and Astrophys.* **523**, A59 (2010).
116. P. J. Huggins, N. Mauron, and E. A. Wirth, *Mon. Not. R. Astron. Soc.* **396**, 1805 (2009).
117. M. L. Leal-Ferreira, W. H. T. Vlemmings, P. J. Diamond, et al., *Astron and Astrophys.* **540**, A42 (2012).
118. N. Koning, S. Kwok, and W. Steffen, *Astrophys. J.* **765**, 92 (2013).